View metadata, citation and similar papers at core.ac.uk
brought to you by CORE
provided by Elsevier - Publisher Connector

Cell Metabolism
Article

Xanthine Oxidoreductase Is a Regulator of Adipogenesis and PPARγ Activity

Kevin J. Cheung,[1,4] Iphigenia Tzameli,[2,4] Pavlos Pissios,[2] Ilsa Rovira,[3] Oksana Gavrilova,[3] Toshio Ohtsubo,[3] Zhu Chen,[1] Toren Finkel,[3] Jeffrey S. Flier,[2] and Jeffrey M. Friedman[1,*]
[1] Laboratory of Molecular Genetics, The Rockefeller University, 1230 York Avenue, New York, NY 10021, USA
[2] Division of Endocrinology, Beth Israel Deaconess Medical Center, Harvard Medical School, Boston, MA 02215, USA
[3] Molecular Biology Section, Cardiovascular Branch, National Heart, Lung, and Blood Institute (NHLBI), Building 10-CRC, Room 5-3330, Bethesda, MD 20892, USA
[4] These authors have contributed equally to this work.
*Correspondence: friedj@mail.rockefeller.edu
DOI 10.1016/j.cmet.2007.01.005

SUMMARY

In an effort to identify novel candidate regulators of adipogenesis, gene profiling of differentiating 3T3-L1 preadipocytes was analyzed using a novel algorithm. We report here the characterization of xanthine oxidoreductase (XOR) as a novel regulator of adipogenesis. XOR lies downstream of C/EBPβ and upstream of PPARγ, in the cascade of factors that control adipogenesis, and it regulates PPARγ activity. In vitro, knockdown of XOR inhibits adipogenesis and PPARγ activity while constitutive overexpression increases activity of the PPARγ receptor in both adipocytes and preadipocytes. In vivo, XOR −/− mice demonstrate 50% reduction in adipose mass versus wild-type littermates while obese *ob/ob* mice exhibit increased concentrations of XOR mRNA and urate in the adipose tissue. We propose that XOR is a novel regulator of adipogenesis and of PPARγ activity and essential for the regulation of fat accretion. Our results identify XOR as a potential therapeutic target for metabolic abnormalities beyond hyperuricemia.

INTRODUCTION

Obesity, defined as an increased adipose tissue mass, is an important public health problem in the developed world and a growing problem in the developing world. While several of the molecular mechanisms that regulate adipocyte development have been elucidated, there is a clear need to more fully define the complex molecular processes that control adipose tissue formation, in an effort to manipulate its accretion. In this report, we set out to identify novel regulators expressed at a very early window during the commitment of a preadipocyte to the adipogenic lineage and with the potential to regulate the activity of proadipogenic factors.

The conversion of a fibroblastic-like preadipocyte to a mature adipocyte involves hormonal stimulators and the induction of a whole network of transcription factors that induce changes in gene expression and cell morphology. At the top of this transcriptional hierarchy are the bzip proteins C/EBPδ, C/EBPβ, C/EBPα, and the nuclear receptor PPARγ (Cao et al., 1991; Yeh et al., 1995). These transcription factors are induced in a sequential and tightly regulated manner, and all are essential for normal adipogenesis. Among them, PPARγ is considered to be the master regulator since it is both necessary and sufficient for adipose differentiation in vitro and in vivo (Evans et al., 2004; Mueller et al., 2002; Rosen et al., 1999; Tontonoz et al., 1994). PPARγ is a ligand-regulated nuclear-hormone receptor that heterodimerizes with the retinoic X receptor (RXR) (Tontonoz et al., 1994) and, upon ligand binding, activates transcription of target genes. Liganded PPARγ and C/EBPβ turn on C/EBPα expression (Zuo et al., 2006), which then acts in concert with PPARγ to induce and maintain adipogenesis via the expression of adipose-specific genes (Freytag et al., 1994; Wu et al., 1999). However, it has been shown that many additional factors regulate adipogenesis either by directly activating adipogenic genes and/or regulating the synthesis of the PPARγ ligand.

In this report, we analyzed the gene-expression profiles of 3T3-L1 cells to identify novel genes pivotal in the adipogenic process. In this analysis, emphasis was given to genes whose expression was limited to the first 24 hr after initiation of differentiation as a means for identifying earlier regulators of the adipogenic process. Candidate genes were ranked based on an algorithm modeling the complexity of each gene-expression profile. Expression profiles were fit to a theoretical model of gene transcription using nonlinear regression and ranked by their goodness of fit. Candidates were further stratified by their expression within the desired time frame. The highest-scoring candidate identified was the enzyme xanthine oxidoreductase (XOR). XOR catalyzes the catabolism of purines such as xanthine and hypoxanthine to uric acid (Berry and Hare, 2004; Harrison, 2002). XOR exists as a homodimer with each subunit composed of iron-sulfur, FAD, and molybdopterin binding domains and can be isolated

in two forms as either xanthine dehydrogenase (XDH) or xanthine oxidase (XO). XDH possesses an additional NAD+ binding site, and oxidation of substrates results in electron transfer to NAD+. In XO, molecular oxygen is used as an electron acceptor resulting in generation of reactive oxygen species (ROS). Under certain conditions, XDH can also function as an NADH oxidase to generate ROS (Sanders et al., 1997). More recently, XOR has been implicated in functions beyond purine metabolism (Berry and Hare, 2004; Vorbach et al., 2002), such as the generation of ROS and consequent tissue injury (Granger et al., 1981; McCord, 1985), the endothelial dysfunction seen in diabetes, in atherosclerosis, hypertension, and congestive heart failure (Alderman and Aiyer, 2004; Amado et al., 2005; Doehner et al., 2001; Landmesser et al., 2002; Patetsios et al., 2001; White et al., 1996). In addition, XOR constitutes a major component of the milk-fat globule membrane, which is secreted in milk. XOR colocalizes with the lipid binding protein adipophilin on the milk-fat globule (McManaman et al., 2002), and in one study global deletion of XOR in mice resulted in defects in fat-droplet secretion (Vorbach et al., 2002). These studies suggest a role for XOR in lipid-droplet export and raise the question of whether this enzyme might oxidize or reduce other substrates that function in the context of lipid metabolism and adipogenesis.

Here we present our results that the enzyme XOR is a novel regulator of the adipogenic process. By means of knockdown and overexpression studies in vitro, we show that XOR lies downstream of C/EBPβ in the cascade of factors that control adipogenesis, and upstream of PPARγ that regulates its activity. In vivo, increased XOR expression and activity correlates with increased fat accumulation and lack of XOR with reduced fat mass. Our observations are novel and link the activity of an enzyme to the activity of an adipogenic transcription factor and thus the adipogenic process. Our results also suggest that adipose tissue XOR may be a contributing factor to the hyperuricemia, atherogenic lipids, and oxidative stress seen in obesity and identify XOR as a potential therapeutic target for such metabolic abnormalities.

RESULTS

XOR Is a High-Scoring Candidate Regulator of Adipogenesis

To identify genes temporally regulated during adipogenesis, we performed microarray analysis of 3T3-L1 preadipocytes, at different time points during differentiation (Soukas et al., 2001).

We developed a novel algorithm to identify temporally regulated genes independent of fold change or expression level for ranking genes. For each gene, the temporal expression profile was fit to a model that defines gene expression as a linear combination of sigmoid functions (Figures S1A–S1C). Best-fit parameters were determined by nonlinear regression. Subsequently, genes were ranked by goodness of fit as determined by their R^2 values. This method of analysis was designed to identify genes with a profile of expression with few transcriptional events, each well modeled by a sigmoid curve.

As an example, PPARγ has a high R^2 value of 0.996, and it was expected that other genes with high R^2 would be good a priori candidates in the regulation of adipogenesis, whereas genes with low R^2 values, such as the ribosomal protein Rps18 ($R^2 = 0.1$) would be poor candidates. From the set of top 40 genes selected by this algorithm, 72% have been previously studied in adipocytes and 10% in the setting of mitochondrial respiration, with the remaining genes uncharacterized (Table S1).

Within the subset of genes with maximal expression at an early time frame, the highest-ranking gene was XOR (Figure 1A), with an R^2 value of 0.999. Microarray analysis of mouse tissues from our laboratory also confirmed highest expression of XOR in white adipose tissue (WAT), followed by liver (L) and muscle (M). Expression was minimal in pancreas (P) and hypothalamus (H) (Figure 1B).

XOR mRNA and Activity Is Transiently Induced during Adipocyte Differentiation In Vitro

We next analyzed XOR expression and activity in 3T3-L1 cells. XOR mRNA expression increased 8-fold during the first 12 hr postinduction and subsequently declined to preinduction levels by day 3. This coincided with a rising expression of aP2, a downstream target of PPARγ and a terminal marker of adipocyte differentiation (Figure 1C).

XOR enzymatic activity was assayed in 3T3-L1 cell lysates that were incubated with the substrate xanthine in the absence (assaying XO activity) or presence of NAD (assaying both XO + XDH activity) in order to generate uric acid. An HPLC assay for uric-acid levels was optimized (Figures S2A–S2C). XDH activity was maximally induced at 24 hr postinduction (Figure 1D), while XO activity remained relatively unchanged.

XOR Levels Correlate with Adipose Mass, and XOR −/− Mice Have Decreased Adiposity

We next assayed XOR expression in the white adipose tissue of 6–8 week old male wild-type (WT), obese *ob/ob* mice, and in *ob/ob* mice treated with leptin over a 12 day time period. XOR expression was elevated 2-fold in *ob/ob* mice relative to WT, and treatment of *ob/ob* mice with leptin reduced XOR mRNA to WT levels (Figure 2A). Similarly, serum uric-acid levels were elevated in *ob/ob* mice relative to WT and normalized by leptin treatment (Figure 2B).

XOR null mice are phenotypically normal at birth but fail to thrive and do not live beyond 6 weeks of age (Ohtsubo et al., 2004; Vorbach et al., 2002). Analysis of adipose stores from 2-week-old WT and XOR −/− mice showed a 12% reduction in body weight in XOR −/− versus +/+ mice (Figure 2C), due to a 50% reduction in adipose content (Figure 2D). Serum analysis in XOR −/− mice showed significantly decreased free fatty-acid concentrations, while no significant differences were evident for glucose and serum triglycerides (Figure 2E). These data suggest that XOR may play a role in promoting in vivo adipogenesis, but it is also possible that the reduced adipose tissue

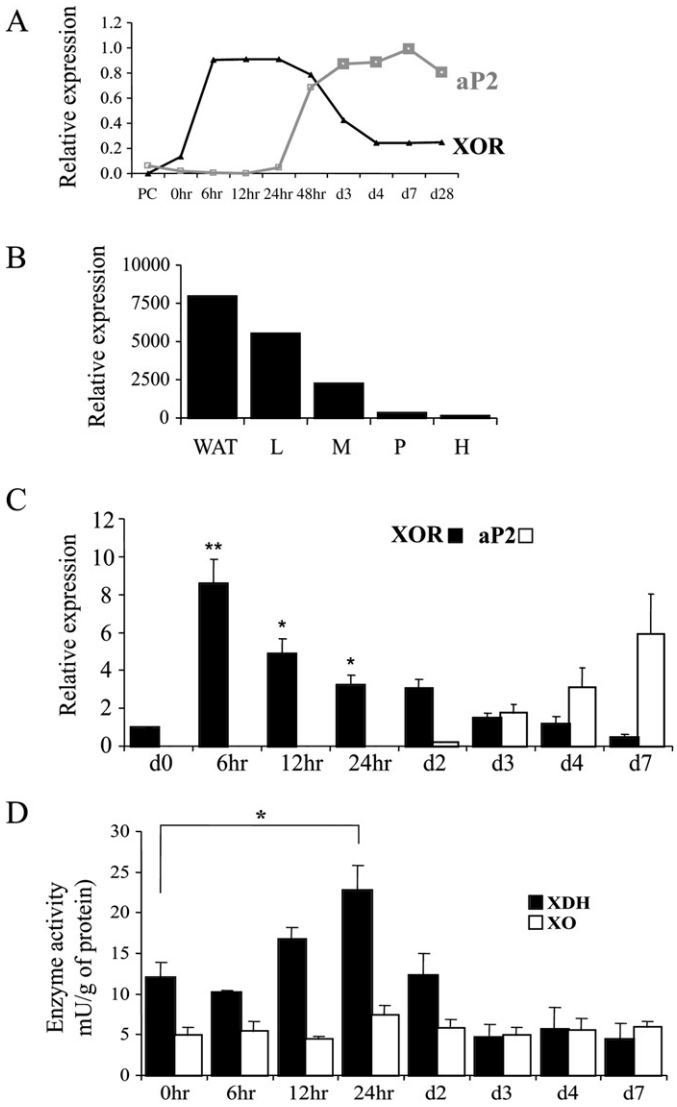

Figure 1. XOR Is a High-Scoring Candidate for Regulation during Adipogenesis

(A) Microarray analysis of XOR (black line) and aP2 (gray line) during 3T3-L1 differentiation.

(B) XOR expression was analyzed using tissue microarray data. XOR expression is highest in white adipose (WAT) and liver (L) and lower in muscle (M), pancreas (P) and hypothalamus (H).

(C) XOR expression during adipogenesis was validated by quantitative RT-PCR. XOR expression is significantly induced between 6–12 hr postinduction, with a subsequent decline (black bars). Decline of XOR expression is coincident with rising aP2 levels (white bars). Data are presented as means ± standard error of the mean (SEM). N = 3–4.

(D) Cell lysates from differentiating 3T3-L1 cells were incubated with xanthine in the absence (XO activity, white bars) or presence of NAD (XO + XDH activity) to generate uric acid. XDH activity (black bars) was maximal at 24 hr postinduction. Data are presented as means ± SEM. N = 3–4.

mass could be secondary to a failure to thrive. To address this, we explored the role of XOR in adipogenesis in vitro and in relation to adipogenic factors.

XOR Expression Is Dependent on the Proadipogenic Transcription Factor C/EBPβ

To explore the determinants of XOR induction during adipogenesis, we titrated the three components of the induction cocktail: insulin, dexamethasone, and the phosphodiesterase inhibitor IBMX. Increasing insulin and dexamethasone concentrations minimally perturbed XOR expression at 6 hr postinduction (Figure S3), whereas increasing concentrations of IBMX proportionally increased XOR gene expression (Figure 3A). Addition of IBMX elevates the intracellular cyclic AMP concentration. Because cAMP induces expression of the proadipogenic transcription factor CCAAT/enhancer binding protein β (C/EBPβ), we considered the possible role of this factor in regulating XOR expression in adipocytes.

Comparison of microarray expression profiles for XOR and C/EBPβ showed a significant correlation (Figure 3B) in the expression pattern of the two genes. To test whether C/EBPβ is necessary for induction of XOR during adipogenesis, 3T3-L1 preadipocytes were retrovirally transfected with two C/EBPβ siRNA constructs and assayed for XOR expression from 6 hr postinduction onward. XOR expression was significantly reduced in the two knockdown cell lines relative to control hairpin (Figure 3C), suggesting that XOR lies downstream of C/EPBβ-dependent pathways.

XOR Is Necessary for Adipogenesis In Vitro, and Knockdown of XOR Inhibits Fat Accumulation

To examine the function of XOR in adipogenesis, short-hairpin siRNA retroviral constructs targeting three regions of the XOR mRNA were generated and stably transfected into 3T3-L1 preadipocytes (Figure 4A). Cells expressing control hairpins differentiated normally, and XOR

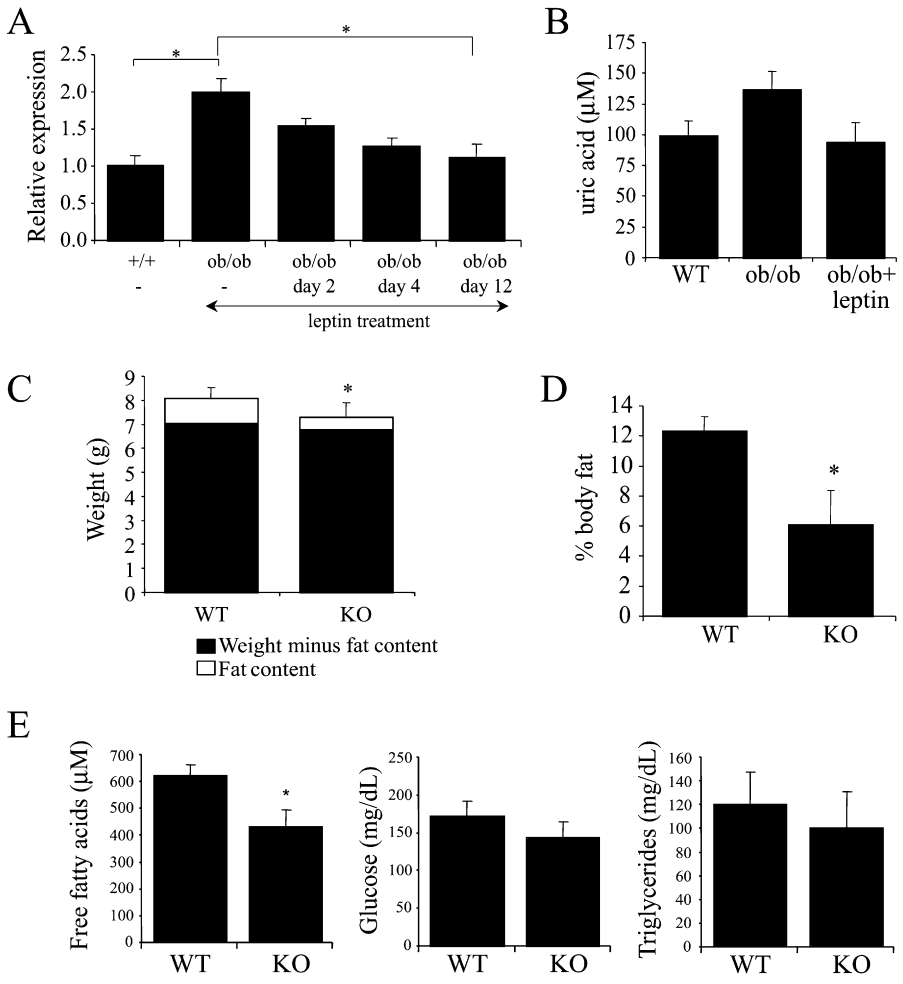

Figure 2. XO Expression and Activity Is Elevated in Obese Mice

(A) XOR expression was assayed in the white adipose tissue of 6- to 8-week-old WT, obese *ob/ob* mice and in *ob/ob* mice treated with leptin over a 12 day time period. N = 2–3.

(B) Serum uric-acid levels are elevated in *ob/ob* mice relative to WT and normalized by leptin treatment. N = 3.

(C) Body weights in 2-week-old male XOR −/− mice (N = 6) and WT littermates (N = 4).

(D) Analysis of adipose tissue content by NMR spectroscopy.

(E) Quantitation of serum-free fatty acids, glucose, and triglycerides. Data in all panels are presented as means ± SEM.

expression was similar to that of untransfected 3T3-L1 cells. XOR expression was significantly reduced by 76% in cell lines derived from construct 1 (XO-1), 53% from construct 2 (XO-2), and 21% in construct 3 (XO-3) (Figure 4A). A reduction in functional enzyme for construct XO-1 was confirmed by HPLC analysis (Figure 4B). The knockdown cell lines were then induced to differentiate, and lipids were stained on day 7 using oil-red-O (Figure 4C). Cells were also assayed for mRNA expression of aP2, a terminal marker of adipogenesis (Figure 4D). A reduced lipid accumulation and aP2 expression was observed for all three constructs, with knockdown XO-1 having the greatest effect. Overall, the efficiency of XOR knockdown in these constructs correlated with the extent of the inhibition of adipocyte differentiation. In addition, expression of C/EBPα, PPARγ, and SREBP1c mRNAs, which normally increase during adipogenesis, was abrogated in XOR-knockdown cells, whereas expression of C/EBPβ mRNA, a putative regulator of XOR, was unaffected (Figure 4E).

XOR is a potent generator of reactive oxygen species with the ability to generate oxidized LDL (oxLDL) in vitro. OxLDL is a source of PPARγ agonists and can induce activation of PPARγ in macrophages (Nagy et al., 1998; Tontonoz et al., 1998). In addition, recent studies have shown production of an endogenous activity during the first 2 days of adipogenesis that activates PPARγ (Tzameli et al., 2004). This reported activation of PPARγ is within the time frame of maximal XOR expression. With this in mind, we wondered if inhibition of XOR blocked adipogenesis by blocking PPARγ activity or acted further upstream of PPARγ. To distinguish between these two possibilities, the PPARγ agonist rosiglitazone was added to control hairpin and XOR-knockdown cells during adipogenesis

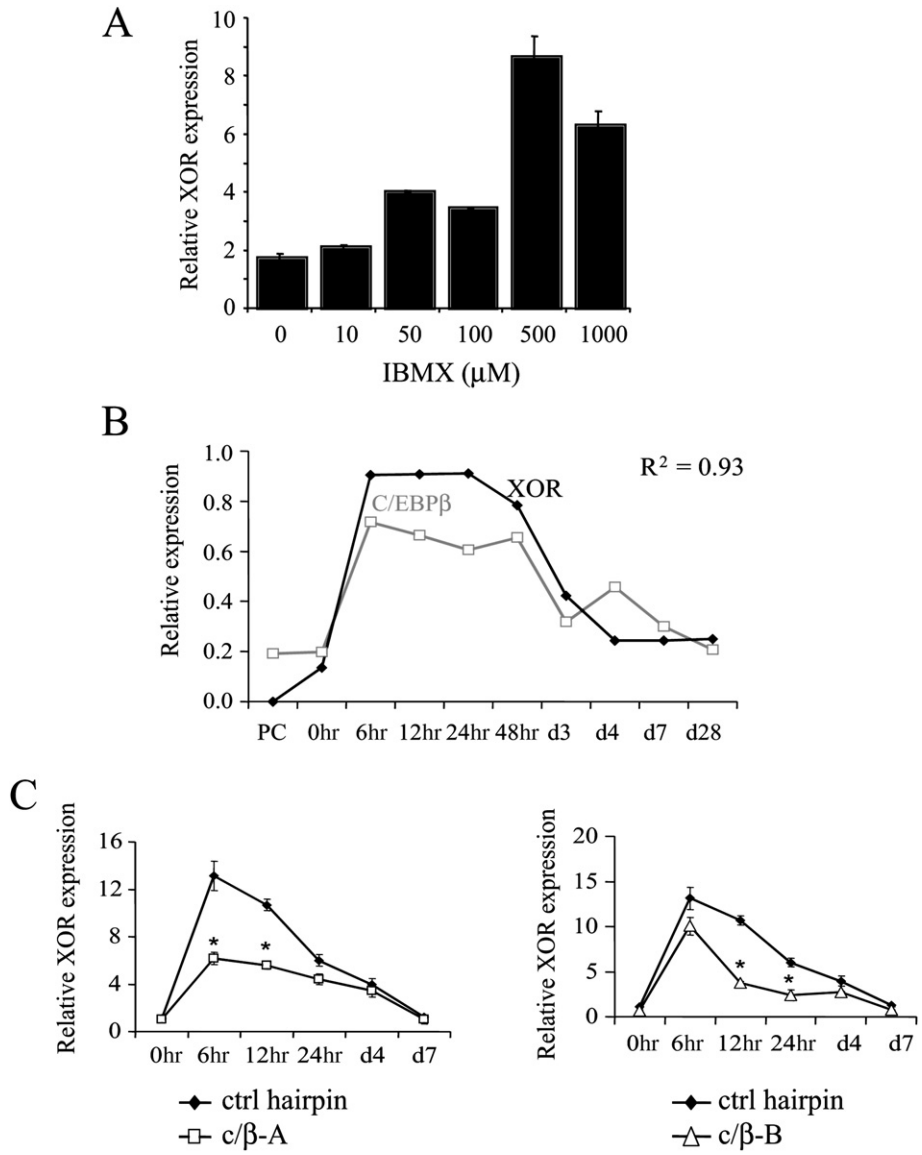

Figure 3. C/EBPβ Is Required for XOR Gene Expression

(A) 3T3-L1 cells were treated with increasing IBMX concentrations at induction of adipogenesis, and XOR expression was assayed at 6 hr postinduction. Data are presented as means ± SEM. N = 2.

(B) Microarray expression profiles as described in Figure 1 were correlated to XOR (black line). Expression of C/EBPβ (gray line) correlated to XOR with Pearson correlation coefficient $R^2 = 0.93$.

(C) Stable 3T3-L1 cell lines infected with C/EBPβ siRNA constructs were assayed for XOR expression at 6 hr postinduction. XOR expression is significantly reduced in the C/EBPβ knockdown cell lines (cβ-A, open square and cβ-B, open triangle) relative to control hairpin (closed diamonds). Data are presented as means ± SEM. N = 2.

(Figure 4F). Rosiglitazone completely rescued adipogenesis in all three XOR-knockdown lines as assayed by oil-red O staining, suggesting that XOR acts upstream of PPARγ and may be involved in the activation of the receptor (Figure 4F).

XOR Is Necessary for PPARγ Activity in 3T3-L1 Cells

PPARγ is activated by a variety of compounds but the identity of the endogenous ligand is unknown. Previous studies have shown that activation of PPARγ in 3T3-L1 cells depends on cAMP and C/EBPβ (Hamm et al., 2001) as well as SREBP1c (Kim et al., 1998) and that production of an endogenous PPARγ ligand (Tzameli et al., 2004) is cAMP dependent. Similarly, XOR expression is induced primarily by the cAMP-inducing agent IBMX and is dependent on C/EBPβ. This line of evidence led us to consider a possible role for XOR in activating PPARγ, either directly or indirectly.

To test this hypohesis, XOR-knockdown constructs were transfected into 3T3-L1 preadipocytes (5B2 cells)

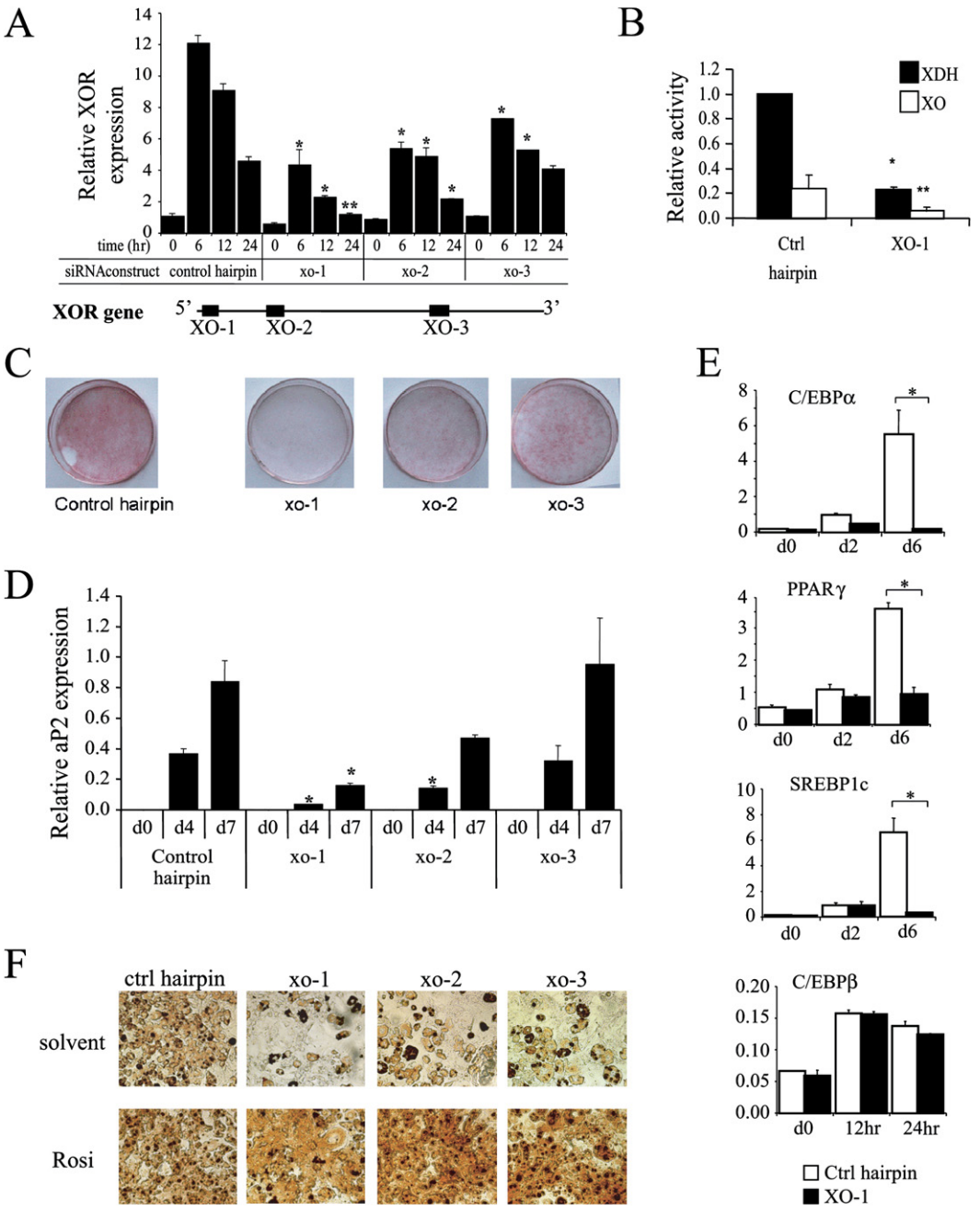

Figure 4. Knockdown of XOR by siRNA Inhibits Adipocyte Differentiation

(A) Retroviral constructs expressing short hairpin RNAs encoding three different XOR regions were used to infect 3T3-L1 preadipocytes. Efficacy of XOR knockdown was tested after induction of differentiation. In control hairpin-expressing cells, XOR expression matches untransfected 3T3-L1. In XOR-knockdown cell lines, XOR expression was significantly reduced in all three constructs. Efficiency of knockdown correlated with the distance from the 5′ end. Data are presented as means ± SEM. N = 2.

(B) XDH (black bar) and XO (white bar) activities are reduced by approximately 80% in XO-1 versus control hairpin cell lines as assayed by HPLC. Data are presented as means ± SEM. N = 3.

(C) Lipid droplets were visualized by oil red O staining, at day 7, in the XOR-knockdown cells.

(D) aP2 expression is most significantly reduced in the XO-1 cells. Data are presented as means ± SEM. N = 2.

(E) C/EBPα, PPARγ, SREBP1c, and C/EBPβ-mRNA levels were measured in the control (white bar) and XO-1 cells (black bar). mRNA levels of all genes are significantly decreased in the XO-1 cells except for C/EBPβ. Statistical analysis was performed by Oneway Anova. Pairwise comparison was done by Tukey-Kramer honestly significant difference (HSD). Data are presented as means ± SEM. N = 3. $p < 0.01$.

(F) Adipogenesis is restored in the XOR-knockdown cells by treatment with 1 μM rosiglitazone (R) from days 0–2 of induction. Cells were stained with oil red O at day 7.

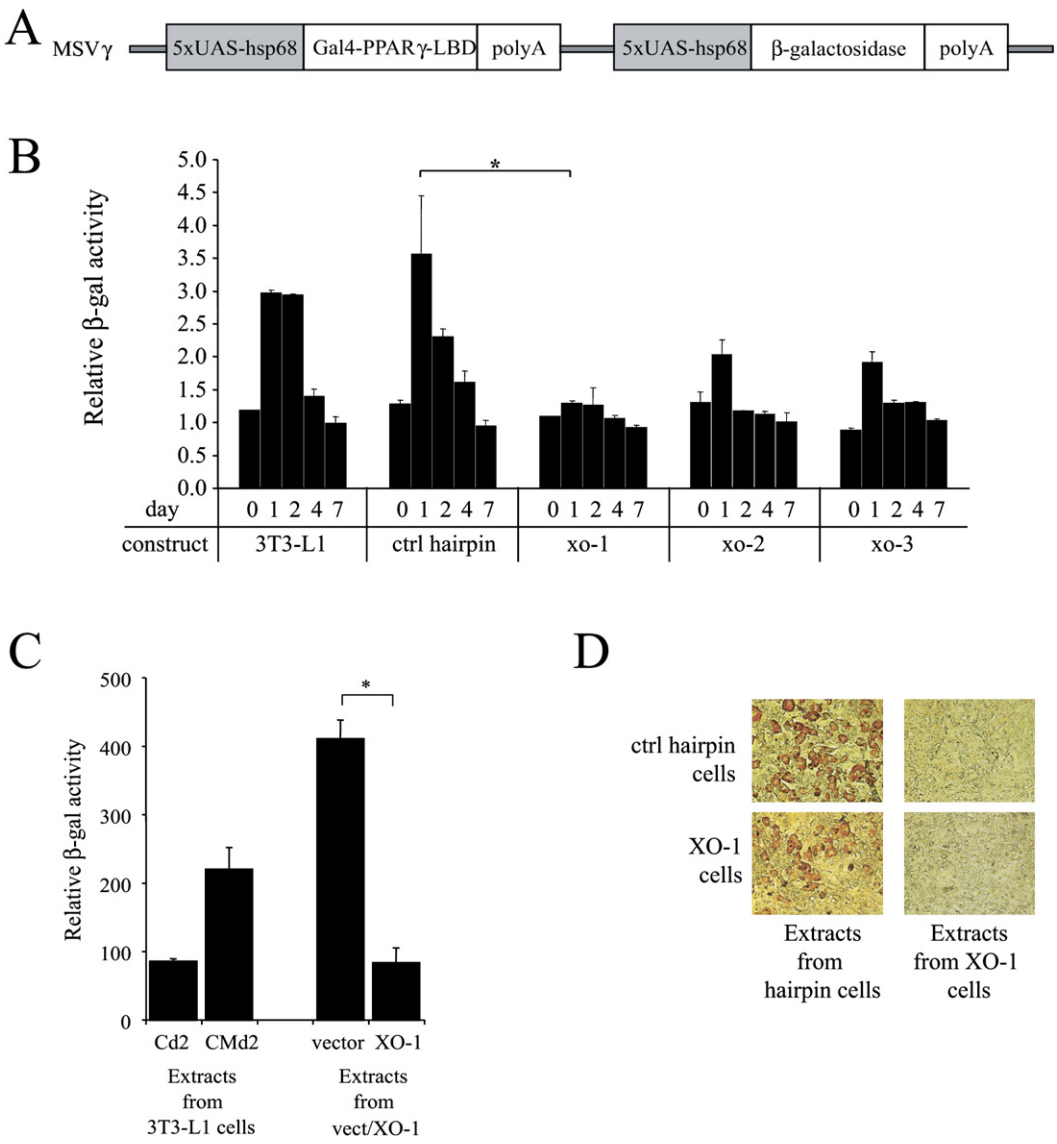

Figure 5. XOR Is Necessary for PPARγ Activity during Adipogenesis

(A) Schematic representation of the MSVγ construct expressed in 5B2 cells.

(B) 5B2 cells were retrovirally infected with XOR-knockdown vectors and assayed for β-gal activity following induction with cocktail. XO-1 knockdown significantly reduced β-gal activity.

(C) Conditioned media from XO-1 and control-hairpin knockdowns collected at day 2 after induction were organically extracted and tested for PPARγ activity on 5B2 cells. Labels are as follows: Cd2, organic extract from noninduced cells; CMd2, organic extract from cocktail-induced cells; Ctrl, organic extract from induced vector-infected cells; and XO-1, organic extract from knockdown-induced cells. Statistical analysis in (B) and (C) was performed by Oneway Anova. Pairwise comparison was done by Tukey-Kramer HSD. Data are presented as means ± standard deviation (SD). N = 3. $p < 0.05$.

(D) Organic extracts from vector and knockdown-induced cells were applied to vector and XO-1-infected 3T3-L1 preadipocytes. Cells were oil red O stained at day 8.

that express a PPARγ ligand-monitoring β-galactosidase (β-gal) reporter (MSVγ). The MSVγ construct encodes both a Gal4-DNA binding domain fused to the PPARγ ligand binding domain (LBD) as well as β-gal as a reporter, on a single plasmid. Expression for both effector and reporter is under the control of five Gal4 specific binding sites (UAS_5) and the hsp68 minimal promoter (Figure 5A). The MSVγ construct thus provides a readout of endogenous PPARγ activity (Tzameli et al., 2004).

Clonal 5B2 preadipocytes expressing MSVγ were retrovirally infected with XOR-knockdown vectors and assayed for β-gal activity following induction with differentiation cocktail (DIM), relative to noninduced cells. Noninduced cells were mock induced with maintenance media.

Beta-gal activity was abrogated in XOR-knockdown cell lines (Figure 5B) and reduction correlated with knockdown efficiency (Figure 4A). At day 1, β-gal activity was reduced by 66% in XO-1, 42% in XO-2, and 45% in XO-3 knockdowns.

Previously, the endogenous PPARγ activity has been shown to accumulate in the organic extract from conditioned media of differentiating 3T3-L1 cells (Tzameli et al., 2004). To assess if XOR regulates the production of such a secreted component as well, media from XOR-knockdown and control-cell lines were organically extracted. The organic extracts were tested for their ability to activate PPARγ and increase β-gal activity by addition to the 5B2 reporter cells (Figure 5C). Organic extract collected from day 2 differentiating 3T3-L1 cells (CMd2) but not extract from noninduced cells (Cd2) increased activity 2.5-fold above baseline. Extracts from 3T3-L1 cells infected with control hairpin vector produced a comparable 4-fold induction, while extracts from XO-1 cells were unable to increase β-gal activity. The same extracts were also tested for adipogenesis and fat accumulation by supplementing them to confluent preadipocytes (Figure 5D). As shown, increased adipogenesis was observed by oil red O staining when organic extracts from control hairpin cells were added to vector-infected cells and XO-1 knockdown cells. On the other hand, extracts from XO-1 knockdown cells were defective in inducing lipid accumulation. Together, these data suggest that XOR enzymatic pathways produce secreted components that activate PPARγ and promote adipogenesis.

Complex Effect of XOR Overexpression on PPARγ Activity and Adipogenesis

Given these results, we sought to determine if overexpression of XOR could enhance PPARγ activation. A retroviral construct encoding human XOR cDNA (*hXOR*) was used to produce 3T3-L1 cells overexpressing hXOR. hXOR cells showed increased expression of hXOR mRNA while inhibiting induction of the endogenous mouse XOR (Figure 6A). hXOR cells also showed a modest 2.5-fold increased in functional enzyme activity as assayed by HPLC (Figure S4).

Overexpression of XOR is implicated in an array of diseases arising from tissue injury and endothelial dysfunction relating to increased ROS generation (Harrison, 2002; Pacher et al., 2006). In addition, exogenous xanthine oxidase is commonly used as a source of superoxide in experimental models of oxidative damage. With this potential complication in mind, we tested the effect of constitutive hXOR overexpression on the ability of the cells to accumulate fat. As shown, hXOR cells showed decreased C/EBPα, PPARγ, and aP2 mRNA expressions (Figure 6A) and reduced fat accumulation (Figure 6B).

Despite the negative effect of XOR overexpression on adipogenesis, there was still an increase in PPARγ activation. Organically extracted conditioned media from vector and hXOR cells, collected at the indicated days after induction of adipogenesis, were tested for their ability to activate PPARγ and increase β-gal activity (Figure 6C). An enhanced PPARγ activation was produced, which was most prominent by hXOR extracts collected at day 4 after differentiation, relative to extracts from vector cells. In addition, all XOR extracts were more potent than vector extracts in inducing fat accumulation (Figure 6D).

We then evaluated the ability of XOR chemical inhibitors to block PPARγ activation and adipogenesis. For this, noninfected and hXOR-infected 5B2 cells were assayed for β-gal activity in the presence of oxypurinol. Oxypurinol, the active form of the XOR-inhibitor allopurinol, was ineffective in inhibiting differentiation-dependent increases in β-gal and therefore PPARγ activity when added to parental (Figure 6E), vector-infected, or hXOR-5B2 cells (Figure 6F). In addition, either 50 or 100 μM oxypurinol were unable to potently inhibit adipogenesis and lipid- droplet formation (Figure 6G). Oxypurinol inhibits the oxidase activity of XOR by binding to the molybdenum site of the enzyme (Spector, 1988), but not its FAD site-dependent dehydrogenase (NADH-oxidizing) activity (Zhang et al., 1998). Given that XOR exists in 3T3-L1 cells mainly as a dehydrogenase (Figure 1D), we sought to find alternative inhibitors. Several reports (Doussiere and Vignais, 1992; Sanders et al., 1997; Zhang et al., 1998) have suggested that diphenyleneiodonium (DPI), a powerful inhibitor of the FAD site of XOR, blocks XOR-mediated reactive oxygen species (ROS) generation from NADH oxidation. Although an inhibitor not exclusive to XOR, we tested DPI in adipogenic and PPARγ activity assays. DPI was able to inhibit PPARγ activity in parental (Figure 6E), vector, and hXOR-overexpressing 5B2 cells (Figure 6F) as well as fat accumulation (Figure 6G). This result suggests that the NADH-oxidizing activity of XOR may be involved in the activation of PPARγ.

Finally, in 5B2 cells overexpressing hXOR, β-gal activity was significantly increased following induction with differentiation cocktail (DIM) (Figure 7A). This increase was up to 150% relative to the control vector cell line and remained elevated nearly 2-fold above baseline through day 6 postinduction. Interestingly, a 2-fold increase of β-gal activity was also observed in 5B2 preadipocytes that did not receive induction cocktail (Figure 7A). In cells treated with 1 μM rosiglitazone for a maximum of 2 days, β-gal activity was increased 5-fold by day 1 and remained elevated to over 7-fold until day 6. The observed potentiation of the rosiglitazone-dependent activation of the reporter system was intriguing, so we sought to analyze it more extensively. For this, we evaluated increases in β-gal activity at day 1, in cells stably expressing hXOR and with concentrations of rosiglitazone ranging from 100 nM to 1 μM. Again, overexpression of hXOR resulted in a 2-fold increase in β-gal activity over that of the vector cells, observed at all concentrations of the agonist (Figure 7B). These results indicate that hXOR enzymatic pathways affect the ligand-dependent transactivation of PPARγ.

In an effort to understand how hXOR affect the ligand-dependent transactivation of PPARγ, we investigated possible XOR-induced changes in the ligand binding domain (LBD) of PPARγ. We performed a trypsin-digestion

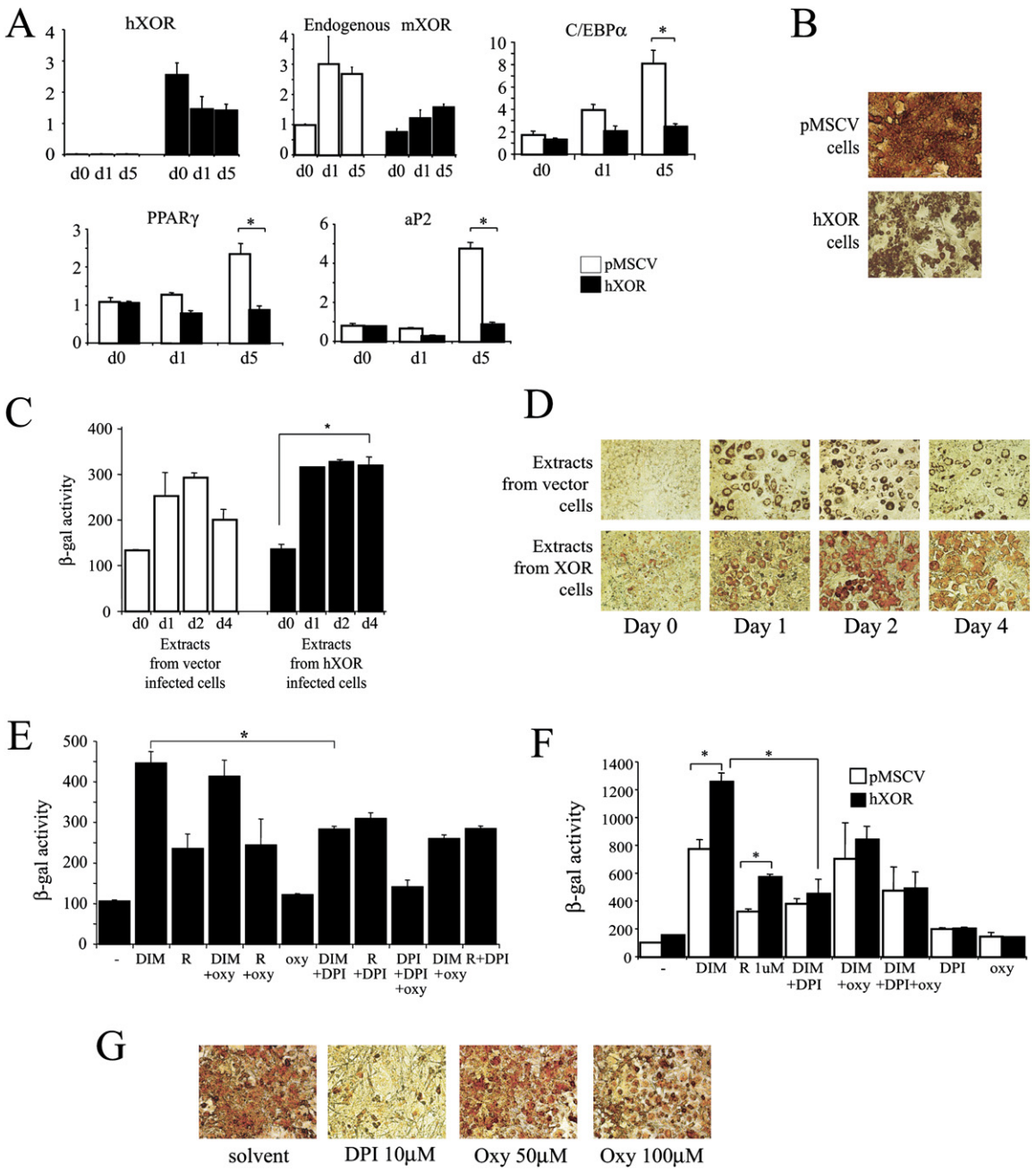

Figure 6. XOR Overexpression Increases PPARγ Activity but Inhibits Adipogenesis

(A) 3T3-L1 cells stably expressing control vector (white bar) or hXOR (black bar) were induced to differentiate. RNA collected at day 0, 1, and 5 after induction was used to assay the levels of hXOR, endogenous mouse XOR, C/EBPα, PPARγ, and aP2.

(B) Vector and hXOR-infected 3T3-L1 cells were induced to differentiate. Cells were stained with oil red O at day 8. Statistical analysis was performed by Oneway Anova. Pairwise comparison was done by Tukey-Kramer HSD. Data are presented as means ± SEM. N = 3. $p < 0.01$.

(C) Conditioned media from vector and hXOR 3T3-L1 cells were collected at day 0, 1, 2, and 4 after adipogenesis and were organically extracted. 5B2 cells were then incubated with these extracts for 24 hr before assayed for β-gal activity.

(D) Organic extracts as described in 6C were applied to 3T3-L1 preadipocytes and assayed for fat accumulation by oil red O staining.

(E) 5B2 cells induced to differentiate with cocktail (DIM) were also treated with 100 μM of oxypurinol (Oxy), 10μM of DPI, 1 μM rosiglitazone, and their combinations. Twenty four hours later, cells were lysed and assayed for β-gal activity. Statistical analysis in (C), (E), and (F) was performed by Oneway Anova. Pairwise comparison was done by Tukey-Kramer HSD. Data are presented as means ± SD. N = 3. $p < 0.05$.

(F) Vector-infected 5B2 cells (white bar) and hXOR-overexpressing 5B2 cells (black bar) were induced to differentiate as in 5C before they were assayed for β-gal activity.

(G) 3T3-L1 cells were induced to differentiate by the standard cocktail in the absence or presence of DPI or oxypurinol. Twenty-four-hour treatment with DPI blocked fat accumulation. Twenty-four-hour treatment with oxypurinol did not inhibit fat accumulation significantly. Cells were stained at day 8.

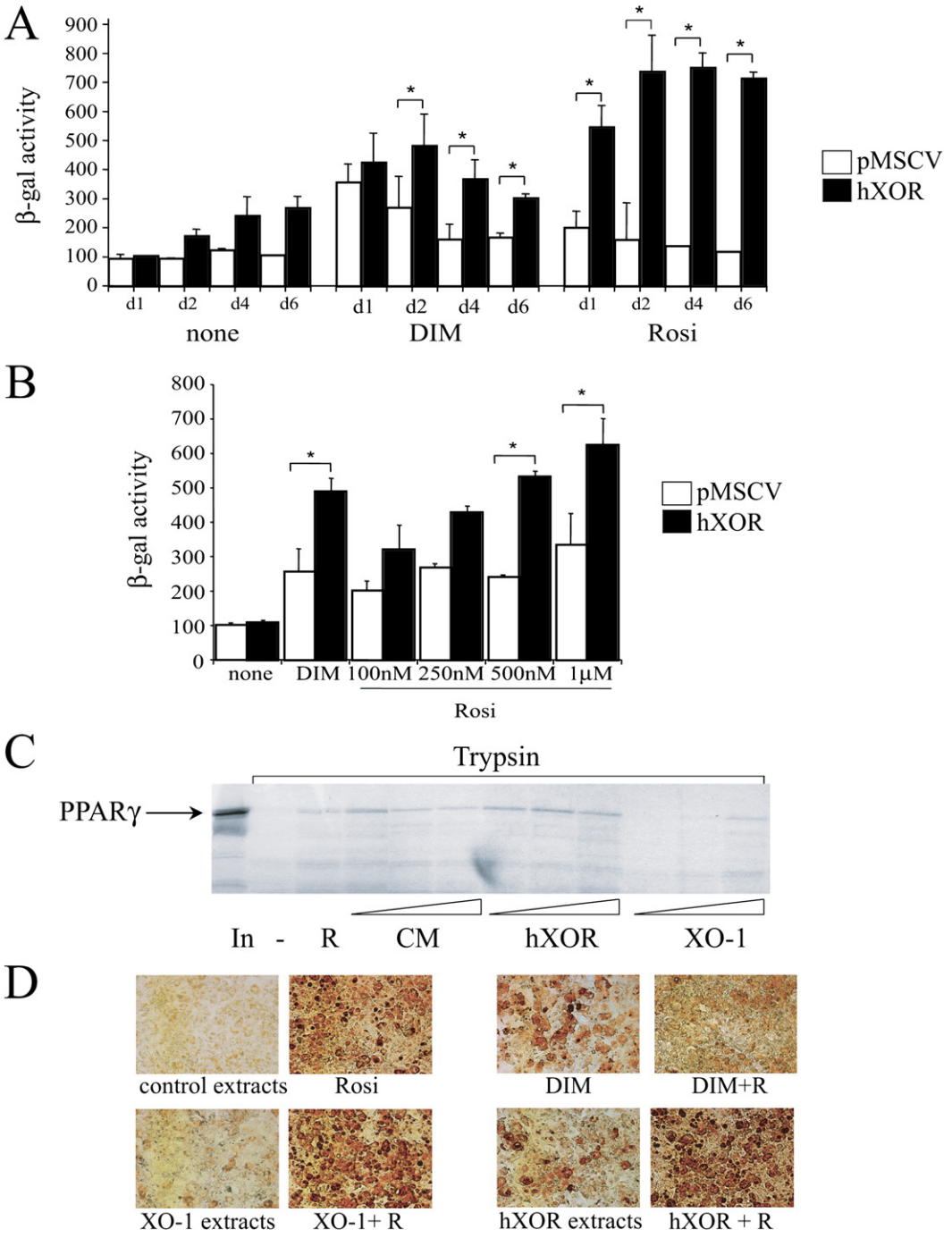

Figure 7. XOR Potentiates Activation of PPARγ by Rosiglitazone and Promotes Fat Accumulation in NIH-3T3

(A) β-Gal activity was measured in vector- and hXOR-overexpressing 5B2 cells at day 1, 2, 4, and 6 postinduction. Labels are as follows: None, no cocktail; DIM, cocktail; Rosi, 1 μM rosiglitazone from days 0–2.

(B) β-Gal activity was measured at day 1, in vector- and hXOR-overexpressing 5B2 cells treated with DIM or increasing amounts of rosiglitazone. Statistical analysis in (A) and (B) was performed by Oneway Anova. Pairwise comparison was done by Tukey-Kramer HSD. Data are presented as means ± SD. N = 3. $p < 0.05$.

(C) ^{35}S-labeled PPARγ was incubated with solvent (−), 1 μM rosiglitazone (R), or increasing amounts of organic extracts from 3T3-L1 (CM), hXOR and XO-1 cells for 30 min. The reactions were treated with trypsin for 7 min and analyzed on a 15% SDS gel. The gel was dried and exposed to film for visualization.

(D) NIH-3T3 cells stably expressing PPARγ2 were induced to differentiate with 1 μM rosiglitazone (R), standard cocktail (DIM) −/+R, XO-1 extracts −/+R, and hXOR extracts −/+R from day 0–2. Lipids were visualized 12 days later.

assay using ^{35}S-labeled full-length PPARγ and organic extracts from parental 3T3-L1 cells, XOR-knockdown and XOR-overexpressing cells. In this assay, ligand binding as well as coactivator or corepressor binding results in stabilization of the LBD and increased resistance to digestion by proteases (Pissios et al., 2000). As shown, extracts from XOR-overexpressing cells protected PPARγ from degradation, whereas extracts from knockdown cells did not (Figure 7C), suggesting that XOR extracts have an effect on the stabilization of the PPARγ LBD.

We then attempted to further investigate the ability of the extracts from knockdown and overexpressing cells to activate PPARγ and, as a consequence, the adipogenic program, in a cell system related to but distinct from 3T3-L1 cells. For this, we infected NIH-3T3 fibroblasts with a PPARγ2-expressing virus and established an NIH-γ2 cell line that we induced to differentiate in response to XOR extracts. As shown in Figure 7D, differentiation cocktail (DIM) and extracts from XOR-overexpressing cells induced fat accumulation in the NIH-γ2 cells to a comparable degree, whereas extracts from XO-1 knockdown cells did not. Rosiglitazone treatment resulted in efficient fat accumulation, and it rescued the adipogenic defect of the XO-1-treated cells. Finally, addition of rosiglitazone to the hXOR extracts resulted in enhanced fat accumulation compared to that achieved by the rosiglitazone + DIM combination. This result suggests that the XOR enzymatic activity produces extractable components with the ability to activate PPARγ in a heterologous system.

DISCUSSION

A better understanding of the full complement of factors required for normal adipogenesis could form the basis for new therapies that directly target the development of adipose tissue mass. Toward this end we employed a novel computational strategy to identify gene products that might play a role in the early phases of adipogenesis. In this report, we used this algorithm to identify XOR as a novel regulator of adipogenesis and fat accretion and present additional evidence implicating XOR in the regulation of PPARγ activity.

XOR is the principal enzyme responsible for oxidation of purine metabolites to uric acid. Hyperuricemia is highly correlated with increased adiposity, obesity, and the metabolic syndrome (Berry and Hare, 2004; Harrison, 2002; Pacher et al., 2006). Serum leptin is also positively associated with uric-acid levels in humans (Fruehwald-Schultes et al., 1999), while weight loss is associated with decreased urate levels and lowered risk of gout, a disease of urate-crystal deposition (Choi et al., 2005). Our results demonstrate that XOR is highly expressed in adipose tissue compared to other tissues (Figure 1B) and that XOR expression, enzymatic activity, and its product urate are all elevated in obese states (Figure 2). Therefore, adipocyte-derived XOR activity may play a direct role in the hyperuricemia associated with obesity.

XOR is necessary for adipogenesis in vitro and analyses of XOR knockout mice suggests that it could also play a role in this process in vivo. To date, two groups have independently described the phenotype of XOR null mice (Ohtsubo et al., 2004; Vorbach et al., 2002). Although both mouse models carry a global deletion of XOR and die perinatally, the two knockout strains have distinct differences in lactation. The mice used in this study lack lactation defects and instead die because of renal displasia (Ohtsubo et al., 2004). Nonetheless, prior to their demise, the XOR-knockout mice show significant reduction in adipose stores versus WT mice, at 2 weeks of age (Figures 2C–2E). Because XOR is significantly induced during in vitro adipogenesis, and siRNA-mediated reduction of XOR inhibits adipocyte differentiation and PPARγ-mediated gene expression (Figure 4), we suggest that XOR deficiency in adipose tissue could be a contributing factor to the perinatal lethality seen in these mice. In contrast to mice, humans with XOR deficiency can be asymptomatic or present with xanthinuria, leading to xanthine calculi in urine and renal failure (Ichida et al., 1997; Levartovsky et al., 2000). The basis for this species difference is not known.

Adipogenesis is characterized by the successive activation of transcriptional factors and their downstream gene targets, resulting in lipid accumulation (Spiegelman and Flier, 2001). These factors, which include C/EBPβ, C/EBPδ, Klf5, and Krox20, among others, ultimately induce activation of PPARγ (Chen et al., 2005; Lane et al., 1999; Oishi et al., 2005). Among them, C/EBPβ is expressed very early following induction of 3T3-L1 preadipocytes, and ectopic expression of C/EBPβ in multipotent NIH-3T3 cells induces PPARγ and fat accumulation (Wu et al., 1995). In addition, loss-of-function studies demonstrate the requirement of this transcription factor for adipogenesis in vitro and in vivo (Chen et al., 2005; Tanaka et al., 1997). Interestingly, overexpression of C/EBPβ in neuronal cells was shown to elevate XOR expression (Cortes-Canteli et al., 2004), and functional C/EBPβ binding sites were recently reported to exist on the rat XOR promoter (Chow et al., 1995). C/EBPβ was also found to activate the mouse XOR promoter in mouse mammary epithelial cells (Seymour et al., 2006). Our results now show that C/EBPβ may also play a role in the regulation of XOR in adipocytes since C/EBPβ knockdown in 3T3-L1 cells results in reduced XOR mRNA (Figure 3C). On the other hand, C/EBPβ-mRNA levels remain unaffected in XOR-knockdown cells (Figure 4E). In aggregate, our findings suggest that XOR may be a downstream target of C/EBPβ and a mediator of C/EBPβ actions in adipogenesis.

While there have been successful efforts to identify the transcription factors that induce expression of PPARγ, much less is known about factors that affect the ligand-dependent activity of the receptor. The evidence in this report indicates that XOR may serve this function. A knockdown of XOR in 3T3-L1 preadipocytes renders them defective in inducing markers of terminal differentiation such as C/EBPα, PPARγ, SREBP1c, and aP2 (Figure 4E) and in accumulating fat (Figure 4F), suggesting that XOR plays a pivotal role during the early event of the process. Adipogenesis is fully restored in the

XOR-knockdown cells by addition of rosiglitazone (Figure 4F), suggesting that this blockage is upstream or at the level of PPARγ activation. An assay able to monitor PPARγ activity in 3T3-L1 cells shows that XOR-knockdown blocks differentiation-dependent PPARγ activation (Figure 5B) and suggests that XOR may be required for the activation of PPARγ. In addition, chemical inhibition of the dehydrogenase activity of the enzyme (Figures 6E and 6F) reduces PPARγ activation, inhibits adipogenesis (Figure 6G), and implicates the NADH-oxidizing activity of XOR and the concomitant generation of ROS in activating PPARγ (Zhang et al., 1998). Overexpression of the enzyme in 3T3-L1 cells increases the β-gal activity of the reporter system even in undifferentiated preadipocytes (Figure 6C) and causes a significant increase in the amount and duration of those secreted components that activate PPARγ and promote adipogenesis (Figure 6D). Finally, a trypsin-digestion assay shows enhanced stabilization of the PPARγ LBD in the presence of extracts from XOR-overexpressing cells, adding further evidence to the conclusion that XOR can stimulate the synthesis of PPARγ ligands and/or cofactors (Figure 7C). This line of evidence initially suggested that XOR might be involved in the synthesis of the elusive PPARγ ligand. For example, XOR is able to oxidize LDL, and such oxLDL particles have been reported to contain PPARγ-ligand-type activities (Nagy et al., 1998; Tontonoz et al., 1998). The observation though that XOR overexpression strongly potentiates the rosiglitazone-dependent activation of PPARγ (Figures 7A and 7B) suggests that the mechanism by which XOR affects PPARγ may be more complex. While the precise mechanism by which XOR increases PPARγ activity is not known, the data suggest that the following mechanisms may contribute: (1) promoting the generation of another endogenous ligand with unique properties, (2) modifying and turning weaker endogenous ligands into high-affinity ones, or (3) promoting changes in the receptor LBD that stabilize binding of endogenous as well as exogenous ligands. Additional experiments are required to clarify this point.

It is also intriguing that the increase in PPARγ activity is not associated with increased adipogenesis in the XOR-overexpressing cells (Figure 6B). As shown here, XOR expression and activity are tightly regulated, with a robust increase during the first 24 hr after initiation of differentiation and then a return to basal levels. It is therefore possible that prolonged presence of XOR, as is often the case for tightly regulated factors expressed outside their natural time window, inhibits adipogenesis.

In summary, we report here that XOR is a novel regulator of adipogenesis and PPARγ activity. Inhibition of its expression and/or enzymatic activity blocks both PPARγ activation and fat accumulation. To our knowledge, there have not been studies designed to explore the effects of XOR inhibitors on body weight, and in light of our findings, such studies may be warranted. Our observations implicate XOR as a regulator of nuclear-hormone receptor activity and identify XOR as a potential therapeutic target for metabolic abnormalities beyond hyperuricemia.

EXPERIMENTAL PROCEDURES

Materials

Methylisobutylxanthine (MIX), insulin, dexamethasone, oil red O, and oxypurinol were from Sigma-Aldrich (St. Louis, MO). The Galacto-Light kit was from Tropix (Foster City, CA), charcoal-dextran stripped serum from Hyclone (Logan, UT), and diphenyleneiodonium and rosiglitazone from Cayman Chemicals.

Microarray Analysis

Microarray data for 3T3-L1 adipogenesis (from Soukas et al., 2001) were analyzed using a novel algorithm. Let g(t) be defined as transcription of a single gene over time. Each gene expression profile g(t) can be expressed as a linear combination of *n* sigmoidal functions $f_i(t)$ from i = 1 to *n*. Best fit parameters were derived from nonlinear regression using SigmaPlot for each g(t). Given the dimensionality of the data set (10 time points), *n* was set at 2. Genes were then ranked by goodness of fit as related to their R^2 values (see Figure S1) with highest R^2 values ranked first.

Retroviral Plasmids and Infections

For knockdown of XOR, we used DNA-based retroviral vector-mediated siRNA technology (Clontech's RNAi-Ready pSIREN-RetroQ system). Targeted sequences were determined by the Whitehead Institute siRNA-designing tool, and specificity was verified by BLAST analysis. Two complementary oligos for each targeted sequence were ligated into the BamHI/EcoRI-linearized pSIREN-RetroQ Vector. Sequences for the antisense oligonucleotides are as follows: XO-1 (positions 2–24) GGTAGACCAGAAGTGTTGT, XO-2 (positions 626–648) CCTGGATCCAGGTCACACG, and XO-3 (positions 3053–3075) CCATCTTGGTGTGAAGGCC.

For overexpression studies, a pcDNA3.1-myc-hisA(−) human-XOR construct (kindly provided by Dr. Toren Finkel) was subcloned into the retroviral pMSCV-hygromycin vector (Clontech). The hXOR gene was excised with 3′ myc and His tags included using NheI and AflII restriction sites, blunt ended, dephosphorylated, and ligated into HpaI cut MSCV-hygro backbone. Plasmids were verified by sequencing.

Recombinant pMSCV or pSIREN-RetroQ viral packaging was achieved by transfection of the plasmids into Phoenix ecotropic packaging cells using Lipofectamine 2000 (Invitrogen). Viral supernatants supplemented with 8 μg/ml polybrene were used to infect 3T3-L1, 5B2, or NIH-3T3 cells for 24–36 hr. Cells were than selected with 2 μg/ml puromycin or 100 μg/ml hygromycin (Sigma).

Infected 5B2 cells were induced to differentiate, and β-gal activity was measured at different time points. Similarly, infected 3T3-L1 and NIH-3T3 cells were induced to differentiate following standard protocols and assayed for lipid content.

Adipocyte Differentiation Assays

3T3-L1 cells (ATCC, Manassas, VA) were maintained in DMEM with 10% FBS (Invitrogen) in 5% CO2. Stable cell lines from retroviral transduction were cultured to confluence and exposed to the differentiation cocktail (1 μg/ml insulin, 0.25 μg/ml dexamethasone, and 0.5 mM IBMX). Forty-eight hours later, cells were switched to medium containing 1 μg/ml insulin until day 7 for harvest. oil red O staining was described previously (Soukas et al., 2001).

Total RNA Extraction and Quantitative RT-PCR

Total RNA was isolated from cells by TRIZOL reagent (Invitrogen). Quantitative RT-PCR was performed by the Taqman system (Applied Biosystems) according to manufacturer's instructions. Oligos were designed by the PrimerExpress software. Threshold cycles (Ct) for the internal control (cyclophilin) and target genes were determined from raw fluorescence. For Figures 4E and 6A, RNA from 3T3-L1 cells was extracted using RNeasy Mini Kit (Qiagen, Valencia, CA) and DNase I treated (Qiagen), according to the manufacturer's instructions. mRNAs were quantitatively measured using a Stratagene MX 4000 Multiplex Quantitative PCR system and single- step quantitative

RT-PCR kit (Stratagene, Cedar Creek, TX). Total RNA was diluted in the range of 0.1–100 ng and used to establish standard curves for each individual gene. Normalization of each mRNA was done by the corresponding TBP mRNA measurement.

XOR Activity and Uric-Acid Assays

Cell lysates were suspended in 50 mM potassium phosphate buffer (pH 7.8) with EDTA and 1X complete protease mini tablet, sonicated, and filtered using a YM-30 centricon filtration device. For the HPLC assays, samples were mixed 1:1 with appropriate 2X buffers for final concentration of 100 μM xanthine + NAD (to assay XDH + XO activity, otherwise XO activity) and also with pyruvate, LDH, and DTE. Samples were then incubated at 37°C for 2–4 hr and acid precipitated with 1% perchloric-acid final concentration. HPLC analysis was done by an HPLC HP1040 system, using a C18 120A DENALI column (Vydac) and isocratic elution with sodium phosphate buffer/1% acetonitrile pH 2.5, with UV detection at A290 nM. Sample absorbance area under the curve was calculated and normalized to UA standard, incubation time, and protein concentration as assayed by Bradford assay. For uric-acid assays, plasma samples from WT, *ob/ob*, and leptin-treated *ob/ob* mice were assayed using a uric-acid SL kit from Diagnostic Chemicals (Oxford, CT).

XOR Knockout Mice Body Composition and Serum Chemistries

Animal care and experimental procedures were performed with approval from the Animal Care and Use Committee of NHLBI under established guidelines. XOR −/− mice were genotyped as described (Ohtsubo et al., 2004). For body composition measurements, 15-day-old male pups were analyzed using a tabletop Bruker Minispec NMR Analyzer mq10 that detects the amount of fat, muscle, and free fluid in nonanesthetized mice. The mice were then anesthetized for blood collection and serum chemistry analysis. The mice were euthanized and the fat pads dissected for quantitation and histological analysis. The fat tissues were fixed on formalin, embedded on paraffin, and mounted on slides for Hematoxylin and Eosin staining (Histoserv, Gaithersburg, MD). Statistical analysis of samples was performed with the two-sample student's t test.

Organic Phase Extraction and Trypsin-Digestion Assay

Conditioned media from 3T3-L1 cells collected at different time points after induction were acidified with 0.1 N HCl, mixed with ethyl acetate:acetone (1:1, v/v), and centrifuged at 1000xg for 5 min. The upper phase was transferred to a new tube, washed twice with NaCl, and evaporated. Dried extracts were reconstituted in DMEM containing 10% stripped-serum FBS and used to treat cells as described previously (Tzameli et al., 2004).

For the protease digestion assay, 2 μl of in vitro translated ^{35}S-labeled PPAR was incubated with EtOH, 1 μM rosiglitazone, or increasing amounts of organic extracts from noninfected differentiating, hXOR-overexpressing, and XO-1-knockdown cells. After a 30 min incubation, 250 ng of trypsin was added to the reaction mixture and protein was digestion at room temperature for 7 min. Reactions were analyzed on a 15% SDS gel, after which the gel was dried and exposed to film (Pissios et al., 2000).

Supplemental Data

Supplemental Data include four figures and one table and can be found with this article online at http://www.cellmetabolism.org/cgi/content/full/5/2/115/DC1/.

Received: July 10, 2006
Revised: November 29, 2006
Accepted: January 16, 2007
Published: February 6, 2007

REFERENCES

Alderman, M., and Aiyer, K.J. (2004). Uric acid: role in cardiovascular disease and effects of losartan. Curr. Med. Res. Opin. *20*, 369–379.

Amado, L.C., Saliaris, A.P., Raju, S.V., Lehrke, S., St John, M., Xie, J., Stewart, G., Fitton, T., Minhas, K.M., Brawn, J., and Hare, J.M. (2005). Xanthine oxidase inhibition ameliorates cardiovascular dysfunction in dogs with pacing-induced heart failure. J. Mol. Cell. Cardiol. *39*, 531–536.

Berry, C.E., and Hare, J.M. (2004). Xanthine oxidoreductase and cardiovascular disease: molecular mechanisms and pathophysiological implications. J. Physiol. *555*, 589–606.

Cao, Z., Umek, R.M., and McKnight, S.L. (1991). Regulated expression of three C/EBP isoforms during adipose conversion of 3T3-L1 cells. Genes Dev. *5*, 1538–1552.

Chen, Z., Torrens, J.I., Anand, A., Spiegelman, B.M., and Friedman, J.M. (2005). Krox20 stimulates adipogenesis via C/EBPbeta-dependent and -independent mechanisms. Cell Metab. *1*, 93–106.

Choi, H.K., Atkinson, K., Karlson, E.W., and Curhan, G. (2005). Obesity, weight change, hypertension, diuretic use, and risk of gout in men: the health professionals follow-up study. Arch. Intern. Med. *165*, 742–748.

Chow, C.W., Clark, M.P., Rinaldo, J.E., and Chalkley, R. (1995). Multiple initiators and C/EBP binding sites are involved in transcription from the TATA-less rat XDH/XO basal promoter. Nucleic Acids Res. *23*, 3132–3140.

Cortes-Canteli, M., Wagner, M., Ansorge, W., and Perez-Castillo, A. (2004). Microarray analysis supports a role for ccaat/enhancer-binding protein-beta in brain injury. J. Biol. Chem. *279*, 14409–14417.

Doehner, W., Rauchhaus, M., Florea, V.G., Sharma, R., Bolger, A.P., Davos, C.H., Coats, A.J., and Anker, S.D. (2001). Uric acid in cachectic and noncachectic patients with chronic heart failure: relationship to leg vascular resistance. Am. Heart J. *141*, 792–799.

Doussiere, J., and Vignais, P.V. (1992). Diphenylene iodonium as an inhibitor of the NADPH oxidase complex of bovine neutrophils. Factors controlling the inhibitory potency of diphenylene iodonium in a cell-free system of oxidase activation. Eur. J. Biochem. *208*, 61–71.

Evans, R.M., Barish, G.D., and Wang, Y.X. (2004). PPARs and the complex journey to obesity. Nat. Med. *10*, 355–361.

Freytag, S.O., Paielli, D.L., and Gilbert, J.D. (1994). Ectopic expression of the CCAAT/enhancer-binding protein alpha promotes the adipogenic program in a variety of mouse fibroblastic cells. Genes Dev. *8*, 1654–1663.

Fruehwald-Schultes, B., Peters, A., Kern, W., Beyer, J., and Pfutzner, A. (1999). Serum leptin is associated with serum uric acid concentrations in humans. Metabolism *48*, 677–680.

Granger, D.N., Rutili, G., and McCord, J.M. (1981). Superoxide radicals in feline intestinal ischemia. Gastroenterology *81*, 22–29.

Hamm, J.K., Park, B.H., and Farmer, S.R. (2001). A role for C/EBPbeta in regulating peroxisome proliferator-activated receptor gamma activity during adipogenesis in 3T3-L1 preadipocytes. J. Biol. Chem. *276*, 18464–18471.

Harrison, R. (2002). Structure and function of xanthine oxidoreductase: where are we now? Free Radic. Biol. Med. *33*, 774–797.

Ichida, K., Amaya, Y., Kamatani, N., Nishino, T., Hosoya, T., and Sakai, O. (1997). Identification of two mutations in human xanthine dehydrogenase gene responsible for classical type I xanthinuria. J. Clin. Invest. *99*, 2391–2397.

Kim, J.B., Wright, H.M., Wright, M., and Spiegelman, B.M. (1998). ADD1/SREBP1 activates PPARgamma through the production of endogenous ligand. Proc. Natl. Acad. Sci. USA *95*, 4333–4337.

Landmesser, U., Spiekermann, S., Dikalov, S., Tatge, H., Wilke, R., Kohler, C., Harrison, D.G., Hornig, B., and Drexler, H. (2002). Vascular oxidative stress and endothelial dysfunction in patients with chronic

heart failure: role of xanthine-oxidase and extracellular superoxide dismutase. Circulation *106*, 3073–3078.

Lane, M.D., Tang, Q.Q., and Jiang, M.S. (1999). Role of the CCAAT enhancer binding proteins (C/EBPs) in adipocyte differentiation. Biochem. Biophys. Res. Commun. *266*, 677–683.

Levartovsky, D., Lagziel, A., Sperling, O., Liberman, U., Yaron, M., Hosoya, T., Ichida, K., and Peretz, H. (2000). XDH gene mutation is the underlying cause of classical xanthinuria: a second report. Kidney Int. *57*, 2215–2220.

McCord, J.M. (1985). Oxygen-derived free radicals in postischemic tissue injury. N. Engl. J. Med. *312*, 159–163.

McManaman, J.L., Palmer, C.A., Wright, R.M., Neville, M.C., Hanson, L., Terada, L.S., Piermattei, D., and Shibao, G.N. (2002). Functional regulation of xanthine oxidoreductase expression and localization in the mouse mammary gland: evidence of a role in lipid secretion. J. Physiol. *545*, 567–579.

Mueller, E., Drori, S., Aiyer, A., Yie, J., Sarraf, P., Chen, H., Hauser, S., Rosen, E.D., Ge, K., Roeder, R.G., and Spiegelman, B.M. (2002). Genetic analysis of adipogenesis through PPARgamma isoforms. J. Biol. Chem. *277*, 41925–41930.

Nagy, L., Tontonoz, P., Alvarez, J.G., Chen, H., and Evans, R.M. (1998). Oxidized LDL regulates macrophage gene expression through ligand activation of PPARgamma. Cell *93*, 229–240.

Ohtsubo, T., Rovira, I.I., Starost, M.F., Liu, C., and Finkel, T. (2004). Xanthine oxidoreductase is an endogenous regulator of cyclooxygenase-2. Circ. Res. *95*, 1118–1124.

Oishi, Y., Manabe, I., Tobe, K., Tsushima, K., Shindo, T., Fujiu, K., Nishimura, G., Maemura, K., Yamauchi, T., Kubota, N., et al. (2005). Kruppel-like transcription factor KLF5 is a key regulator of adipocyte differentiation. Cell Metab. *1*, 27–39.

Pacher, P., Nivorozhkin, A., and Szabo, C. (2006). Therapeutic effects of xanthine oxidase inhibitors: renaissance half a century after the discovery of allopurinol. Pharmacol. Rev. *58*, 87–114.

Patetsios, P., Song, M., Shutze, W.P., Pappas, C., Rodino, W., Ramirez, J.A., and Panetta, T.F. (2001). Identification of uric acid and xanthine oxidase in atherosclerotic plaque. Am. J. Cardiol. *88*, 188–191.

Pissios, P., Tzameli, I., Kushner, P., and Moore, D.D. (2000). Dynamic stabilization of nuclear receptor ligand binding domains by hormone or corepressor binding. Mol. Cell *6*, 245–253.

Rosen, E., Sarraf, P., Troy, A.E., Bradwin, G., Moore, K., Milstone, D.S., Spiegelman, B.M., and Mortensen, R.M. (1999). PPAR gamma is required for the differentiation of adipose tissue in vivo and in vitro. Mol. Cell *4*, 611–617.

Sanders, S.A., Eisenthal, R., and Harrison, R. (1997). NADH oxidase activity of human xanthine oxidoreductase–generation of superoxide anion. Eur. J. Biochem. *245*, 541–548.

Seymour, K.J., Roberts, L.E., Fini, M.A., Parmley, L.A., Oustitch, T.L., and Wright, R.M. (2006). Stress activation of mammary epithelial cell xanthine oxidoreductase is mediated by p38 MAPK and CCAAT/enhancer-binding protein-beta. J. Biol. Chem. *281*, 8545–8558.

Soukas, A., Socci, N.D., Saatkamp, B.D., Novelli, S., and Friedman, J.M. (2001). Distinct transcriptional profiles of adipogenesis in vivo and in vitro. J. Biol. Chem. *276*, 34167–34174.

Spector, T. (1988). Oxypurinol as an inhibitor of xanthine oxidase-catalyzed production of superoxide radical. Biochem. Pharmacol. *37*, 349–352.

Spiegelman, B.M., and Flier, J.S. (2001). Obesity and the regulation of energy balance. Cell *104*, 531–543.

Tanaka, T., Yoshida, N., Kishimoto, T., and Akira, S. (1997). Defective adipocyte differentiation in mice lacking the C/EBPbeta and/or C/EBPdelta gene. EMBO J. *16*, 7432–7443.

Tontonoz, P., Hu, E., Graves, R.A., Budavari, A.I., and Spiegelman, B.M. (1994). mPPAR gamma 2: tissue-specific regulator of an adipocyte enhancer. Genes Dev. *8*, 1224–1234.

Tontonoz, P., Nagy, L., Alvarez, J.G., Thomazy, V.A., and Evans, R.M. (1998). PPARgamma promotes monocyte/macrophage differentiation and uptake of oxidized LDL. Cell *93*, 241–252.

Tzameli, I., Fang, H., Ollero, M., Shi, H., Hamm, J.K., Kievit, P., Hollenberg, A.N., and Flier, J.S. (2004). Regulated production of a peroxisome proliferator-activated receptor-gamma ligand during an early phase of adipocyte differentiation in 3T3-L1 adipocytes. J. Biol. Chem. *279*, 36093–36102.

Vorbach, C., Scriven, A., and Capecchi, M.R. (2002). The housekeeping gene xanthine oxidoreductase is necessary for milk fat droplet enveloping and secretion: gene sharing in the lactating mammary gland. Genes Dev. *16*, 3223–3235.

White, C.R., Darley-Usmar, V., Berrington, W.R., McAdams, M., Gore, J.Z., Thompson, J.A., Parks, D.A., Tarpey, M.M., and Freeman, B.A. (1996). Circulating plasma xanthine oxidase contributes to vascular dysfunction in hypercholesterolemic rabbits. Proc. Natl. Acad. Sci. USA *93*, 8745–8749.

Wu, Z., Xie, Y., Bucher, N.L., and Farmer, S.R. (1995). Conditional ectopic expression of C/EBP beta in NIH-3T3 cells induces PPAR gamma and stimulates adipogenesis. Genes Dev. *9*, 2350–2363.

Wu, Z., Rosen, E.D., Brun, R., Hauser, S., Adelmant, G., Troy, A.E., McKeon, C., Darlington, G.J., and Spiegelman, B.M. (1999). Cross-regulation of C/EBP alpha and PPAR gamma controls the transcriptional pathway of adipogenesis and insulin sensitivity. Mol. Cell *3*, 151–158.

Yeh, W.C., Cao, Z., Classon, M., and McKnight, S.L. (1995). Cascade regulation of terminal adipocyte differentiation by three members of the C/EBP family of leucine zipper proteins. Genes Dev. *9*, 168–181.

Zhang, Z., Blake, D.R., Stevens, C.R., Kanczler, J.M., Winyard, P.G., Symons, M.C., Benboubetra, M., and Harrison, R. (1998). A reappraisal of xanthine dehydrogenase and oxidase in hypoxic reperfusion injury: the role of NADH as an electron donor. Free Radic. Res. *28*, 151–164.

Zuo, Y., Qiang, L., and Farmer, S.R. (2006). Activation of CCAAT/enhancer-binding protein (C/EBP) alpha expression by C/EBP beta during adipogenesis requires a peroxisome proliferator-activated receptor-gamma-associated repression of HDAC1 at the C/ebp alpha gene promoter. J. Biol. Chem. *281*, 7960–7967.

Accession Numbers

The data discussed in this publication have been deposited in NCBIs Gene Expression Omnibus (GEO, http://www.ncbi.nlm.nih.gov/geo/) and are accessible through GEO Series accession number GSE6795.